17 Imaging of Cardiac and Paracardiac Masses and Pseudotumors

BERND J. WINTERSPERGER, MD

INTRODUCTION

Although the use of computed tomography (CT) in cardiac imaging mainly focuses on coronary artery disease and its sequelae, there are many more indications in which CT can provide excellent and valuable information. This has already been reported based on studies with electron beam CT (EBCT). The rapidly emerging and vastly growing interest and knowledge in cardiac CT today is mainly caused by the development and widespread use of multidetector-row CT (MDCT) systems. Initially introduced in 1992 (Elscint CT-Twin), MDCT led to a more widespread use of CT in cardiac imaging, starting with 4-row MDCT. Within recent years, further technical developments have led to the use of 8-, 16-, and 64-row MDCT systems. Cardiac imaging has been one of the major and most exciting focuses of MDCT since then. Although the focus of interest in cardiac MDCT is again coronary artery disease and its prevention, most of the information provided by EBCT can also be revealed by MDCT *(1–4)*.

Compared to other referrals, imaging of cardiac or paracardiac masses is a rather rare request for a CT study. The examination of and screening for cardiac tumors is among the rare causes for performing cross-sectional cardiac imaging studies. The modality of choice in screening for cardiac masses is still 2D echocardiography *(5–7)*. Because of its real-time approach, echocardiography can detect cardiac and even small cardiac valve-attached masses and their impact on valve and global cardiac function within the same examination *(8)*. However, there are certain restrictions to echocardiography affecting its clinical use. Although echocardiography can be easily performed in any patient with bedside capabilities, image quality is mainly dependent on the patient's habitus and the examiner's skills. Besides restrictions caused by limited acoustic windows due to obesity, right-ventricle assessment may be hampered by pulmonary emphysema. In addition, tissue characterization is often not possible even though tumors may present with typical echocardiographic signs. EBCT and MDCT are cross-sectional techniques for acquiring images with high spatial and temporal resolution to freeze cardiac motion and to follow the cardiac cycle *(9,10)*. Although tumor studies are not the primary focus of cardiac CT imaging, CT is a valuable tool in the work-up of patients with suspected cardiac tumors.

As noninvasive cross-sectional imaging modalities, EBCT and MDCT offer a large field of view without major limitations based on the patient's constitution. In addition, with the use of retrospectively electrocardiogram (ECG)-gated data acquisition techniques, MDCT provides a 3D data set that enables secondary reconstruction of any desired image plane. These features overcome the limitation of providing only transaxial images in CT or the approximation of individual cardiac axes in EBCT. With the recent advent of 16-row MDCT, even submillimeter collimated images are possible within a short breath-hold of 17–20 s. However, temporal resolution of EBCT is superior to that of MDCT and also allows visualizing very tiny valve-attached tumors, although this still remains a challenge *(11)*.

IMAGING TECHNIQUES

CT imaging of cardiac masses is basically not different from other cardiac applications like coronary artery imaging or cardiac morphology in congenital heart disease (CHD). Detailed information and background about cardiac CT imaging algorithms using EBCT and MDCT can be found in Part II, "Technical Background."

However, depending on the individual scanner and data acquisition settings, a few basics have to be considered for imaging of cardiac masses.

DATA ACQUISITION

Especially in MDCT cardiac imaging, different algorithms and data acquisition techniques can be used. However, to allow a 3D assessment of the heart with adaptation to individual cardiac axis cardiac chambers, retrospective ECG-gated algorithms are strongly recommended, although they basically lead to a higher radiation exposure. Recently developed techniques allow again for a subsequent reduction of redundant radiation without losing the benefits of retrospective gating. In the assessment of coronary artery calcifications, Jakobs et al. showed a significant reduction of 45–50% without change in image quality *(12)*. As there are major differences in basic techniques, only general recommendations can be given. Technical backgrounds and imaging algorithms of EBCT and MDCT are

From: *Contemporary Cardiology: CT of the Heart: Principles and Applications*
Edited by: U. Joseph Schoepf © Humana Press, Inc., Totowa, NJ

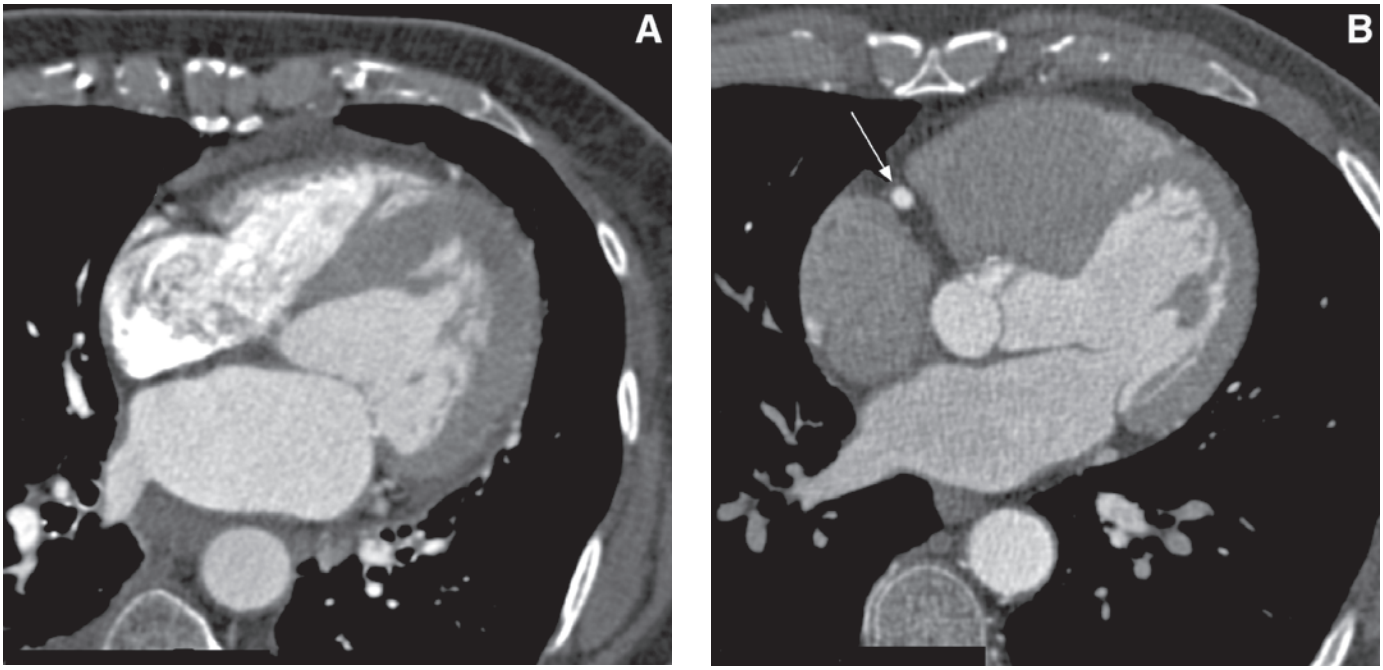

Fig. 1. Axial multidetector-row CT (MDCT) image of a 4-row MDCT scanner system showing artifacts within the right atrium and ventricle due to contrast influx **(A)**. By optimization of contrast application using 16-row MDCT these artifacts can be avoided, leading to a better depiction of the right coronary artery (arrow). However, for mass depiction, an enhancement of all cardiac chambers would be necessary.

substantially different. This implies differences in the exact scanning protocol used. However, there are basic demands and requirements for assessment of cardiac masses in CT that determine the details of the imaging protocol.

MDCT allows for very thin collimated slices in the range of 1 mm or even less. This is favorable for the assessment of coronary arteries but is usually unnecessary for the assessment of cardiac masses. This can also satisfactorily be done with a slice thickness in the range of 2–3 mm. This allows for a cutoff in data acquisition time that makes it even possible to be performed easily within a short breath-hold on 4-row MDCT. With overlapping slice reconstruction, multiplanar reformations (MPR) can be used to determine the exact location and extent of tumors.

Although infrequently used at present, dynamic ECG-triggered or -gated scanning can provide dynamic tumor enhancement and may provide further information concerning tumor type. However, to date there has been no study published focusing on such an imaging strategy in CT.

CONTRAST APPLICATION

Although some features of cardiac tumors (e.g., fatty tissue, calcifications) may even be visible on plain scans without application of contrast agents, allocation of these features and mass diagnosis necessitates the use of iodinated contrast media. There is extensive literature on the optimization of contrast injection regimens, primarily focusing on the assessment of coronary arteries. With the use of 16-row MDCT, contrast agent volume could be reduced, therefore avoiding streak artifacts from high contrast influx within the right atrium and ventricle affecting the assessability of the proximal right coronary artery *(10)* (Fig. 1A,B). However, using these injection protocols, opacfication of the right atrium and ventricle is not guaranteed and mass diagnoses may fail.

Therefore, modification of injection protocols is necessary in order to ensure opacification of all cardiac chambers. Especially where right atrial tumors are suspected, additional delayed scanning during the second or third pass of contrast media will improve the homogeneity of atrial opacification and help to avoid misinterpretation of influx of nonopacified blood from the inferior vena cava.

EPIDEMIOLOGY OF CARDIAC MASSES

Basically, when talking about cardiac masses, primary and secondary tumors have to be differentiated. Primary tumors typically originate within the heart, whereas secondary tumors most commonly result from metastasis of malignancies primarily located outside the heart or from direct tumor spread and invasion of masses located adjacent to the heart (e.g., bronchgenic carcinoma). Primary tumors of the heart are by far less common that secondary tumors. Autopsy studies report a prevalence of primary masses in the range of 0.0017%–0.33% *(13)*. However, although there is a wide range of variation between different studies mainly based on the year of publication and inclusion criteria, primary cardiac masses can definitely be considered as rare tumors when compared to other types. Secondary cardiac tumors on the other hand are about 20–40 times more frequent than primary ones *(13)*. Modern noninvasive imaging modalities such as echocardiography in particular, but also CT and magnetic resonance imaging (MRI), now allow mass diagnosis prior to death and allow for therapy planning. In addition to real neoplasms, no matter whether benign or malignant, primary, or secondary, CT imaging is also increasingly performed when cardiac thrombi are suspected. In

Table 1
Frequency of Benign Cardiac Tumors (adapted from ref. *13*)

Benign tumors	*Approximate frequency (%)*
Myxoma	29
Papillary fibroelastoma	8
Rhabdomyoma	5
Fibroma	5
Hemangioma	4
Lipoma	4
Others	8
Total	63

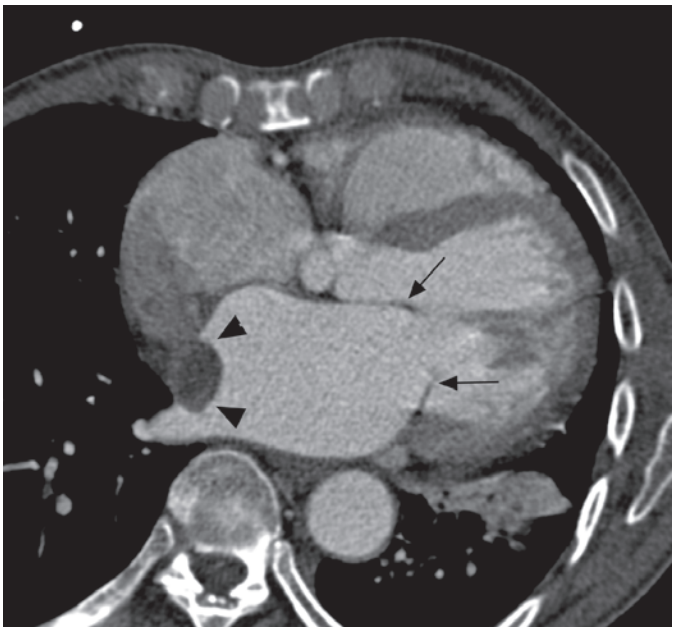

Fig. 2. Patient with a hypodense round mass within the left atrium attached to the interatrial septum (arrow heads). Mass was proven as a myxoma at surgery. Reconstruction was performed during mid-diastole with open mitral valve leaflets (arrows).

addition to imaging features and appearance, cardiac masses can often be differentiated based on location and morphology.

BENIGN CARDIAC TUMORS

Approximately 60–70% of primary cardiac tumors are benign *(13)*. Cardiac myxoma accounts for about half of all benign tumors, followed by papillary fibroelastoma, fibroma, and lipoma (Table 1) *(13)*. However, there is also a difference in frequency of benign tumors based on a patient's age. Whereas myxoma represents the most common tumor type in adults, in childhood, rhabodomyoma accounts for the majority of cases.

Myxomas can be found in all cardiac chambers; however, in approx 75% of the cases, the mass is located within the left atrium (Fig. 2). Another 20% of myxomas are located within the right atrium, whereas only 5% arise within either the left or the right ventricle. In rare instances, myxomas can be found at multiple locations within the heart. Although most cases of cardiac myxoma are sporadic, possibly part of the Carney complex, an autosomal dominant syndrome of cardiac myxomas has been associated with a variety of hyperpigmented skin lesions *(14)*. Also, the development of other, extracardiac tumors and endocrine abnormalities may occur *(15)*.

Although the diagnosis can be easily made using different imaging modalities, patients with cardiac myxoma can be symptomatic for a long time before myxomas are considered as a potential differential diagnosis *(16)*. Patients may present with a triad of symptoms including constitutional symptoms, signs of valvular obstruction (based on myxoma prolapse), and embolic events. The target vasculature of embolic events is strongly dependent on the location of the tumor. Embolic phenomena of left-sided myxomas, considered the most severe complication, may lead to ischemia of either the extremities or the viscera. In case of supra-aortic emboli, symptoms of acute stroke, transient ischemic attacks, or seizures may occur. In right atrial myxomas, symptoms are less frequent.

Atrial myxoma often shows a pedunculated appearance, with its origin in the area of the oval fossa, although the stalk may not be identified with CT (Fig. 3A,B). With increasing size, those mobile masses can even prolapse into the mitral annulus, leading to changes in cardiac hemodynamics. Right-sided myxomas are less frequently attached to the oval fossa. Myomas can even present as a mass within the area of the oval fossa extending to both atria.

Intracavitary tumor masses usually appear as filling defects within the opacified blood pool (Figs. 2 and 3). This necessitates homogeneous contrast distribution and cavitary opacification. However, especially within the right atrium, inflow artifacts need to be differentiated. Mass appearance in CT is strongly dependent on gross pathologic features. Based on their gelatinous nature, myxomas usually have heterogeneous low attenuation at CT (Figs. 2 and 3). Regressive changes may lead to recurrent hemorrhage and calcification, which is frequently seen in CT *(17)* (Fig. 3A). In addition, adherent thrombi can occur. The mobility of myxomas can be demonstrated by either the cine mode in EBCT or multiple data reconstructions at different time points of the cardiac cycle in MDCT with retrospective ECG gating.

Although papillary fibroelastomas represent the second most common benign primary cardiac neoplasm, they are rarely demonstrated with CT modalities. They usually appear at endocardial surfaces and are most commonly located (90%) on valve surfaces. The vast majority of these tumors are less than 1 cm in diameter *(18)*. Their appearance on the rapidly moving valves and their small size makes it rather difficult to identify those lesions using CT, although they are easily detected at echocardiogaphy. Whereas MDCT techniques currently cannot easily follow valve movement because of the rather bad temporal resolution (approx 100–250 ms), EBCT may allow the depiction of those tumors *(11)* (Fig. 4). Recently published MDCT data report the depiction of even small valvular pathology *(19,20)*. However, at present, especially in diagnosis of fibroelastomas, echocardiography is usually far superior to CT. Although symptoms are less frequent than in cases of myxoma, papillary fibroelastomas may also lead to embolic events. This is mostly based on adherent thrombo-embolic material. Although the suspicion of a fibroelastoma cannot be consid-

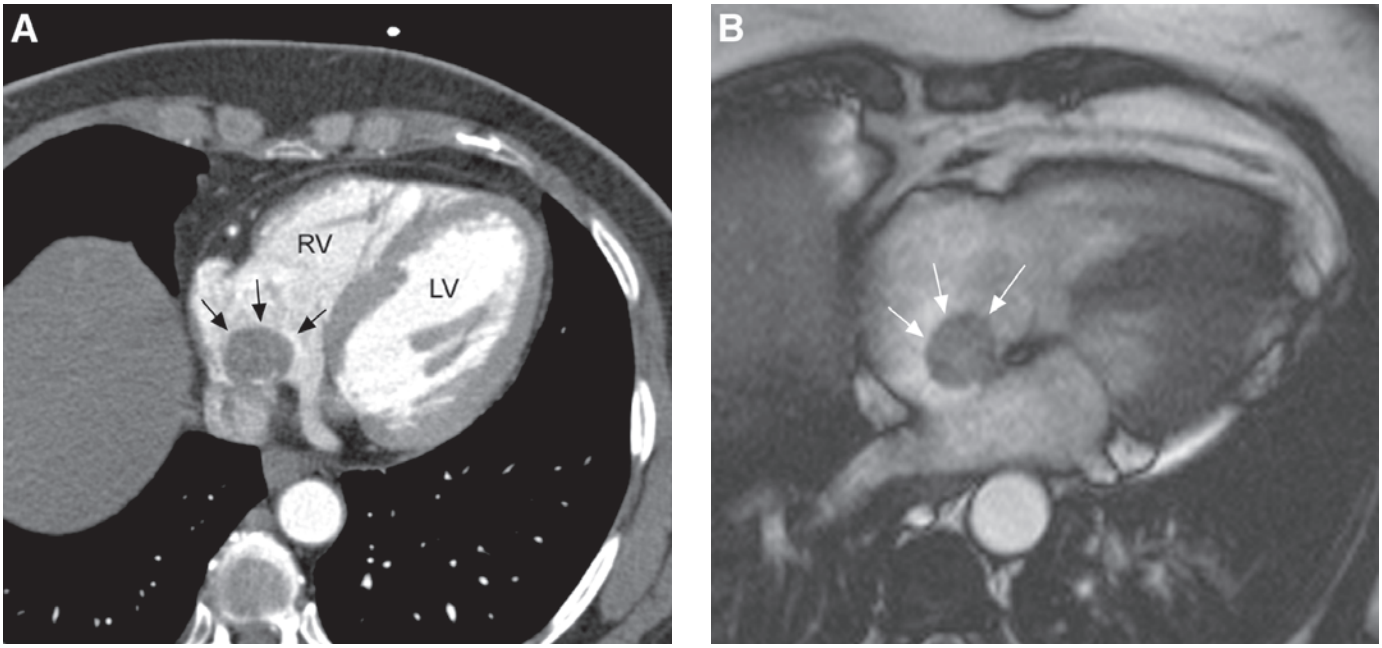

Fig. 3. (A) Round-shaped myxoma of the right atrium with small calcifications (arrows). RV, right ventricle; LV, left ventricle. **(B)** Corresponding magnetic resonance imaging in long-axis orientation show the stalk of the myxoma (arrows) attached to the oval fossa.

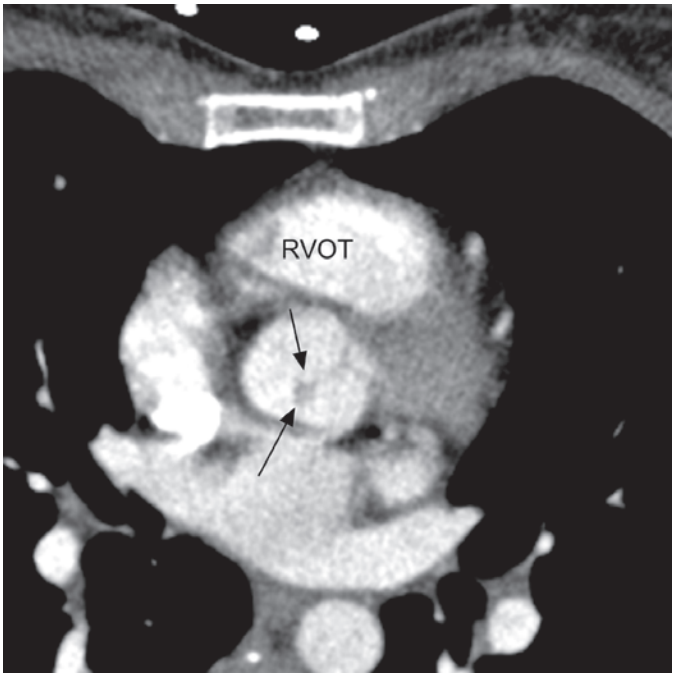

Fig. 4. Axial image of an electron beam CT data set at the level of the aortic valve. A small papillary fibroelastoma can be depicted at the tip of the aortic valve cusps (arrows). RVOT, right-ventricular outflow tract.

ered as a reason for cardiac CT scanning, CT may be helpful to exclude thrombi within the cardiac cavities.

Based on the typical appearance of fatty tissue, lipomatous tumors are usually easily diagnosed using CT. Based on pathology findings, two different types have to be differentiated—lipomas and lipomatous hypertrophy of the interatrial septum.

Contrary to other tumors, lipomas are usually found on the epicardial surface, and may present at any site of the atria or ventricles. However, lipomas may also extent intracavitary. In combination with other tissues, e.g., in angiolipoma, typical image features of fatty tissue may disappear and therefore hamper diagnosis (Figs. 5A–C and 6A,B).

Lipomatous hypertrophy of the interatrial septum consists of an accumulation of mature fat as well as of adipose cells resembling brown fat cells. Deposits at the level of the oval fossa with a diameter larger than 2 cm are considered lipomatous hypertrophy (Fig. 7). These changes may be accompanied by arrhythmias. Similar to lipomas, lipomatous hypertrophy usually shows typical homogeneous low attenuation at CT, which can be found even in nonenhanced scans *(21,22)*.

Other benign tumors such as rhabdomyoma and fibroma usually appear within the ventricular wall or the interventricular septum. They usually show a density comparable to normal myocardium, which precludes easy diagnosis and delineation. Rhabdomyoma is the most frequent tumor in infancy and childhood, and is often associated with tuberous sclerosis *(23)*. Up to 50% of patients with rhabdomyoma suffer from tuberous sclerosis syndrome, and 60% of children with tuberous sclero-

Fig. 5. (A) *(right and page 176)* Axial slices of an extensive mass arising from the right atrial roof, narrowing the right pulmonary artery and the superior vena cava. The mass shows heterogeneous enhancement with central necrosis and calcifications. The mass was proven to be a benign angiomyolipoma based on several tissue probes using CT-guided needle biopsy and open thoracotomy. **(B)** The sagittal reconstruction also shows central necrosis and calcification (arrow). VC, vena cava. Fatty tissue is found only at the very bottom of the mass (arrow heads).

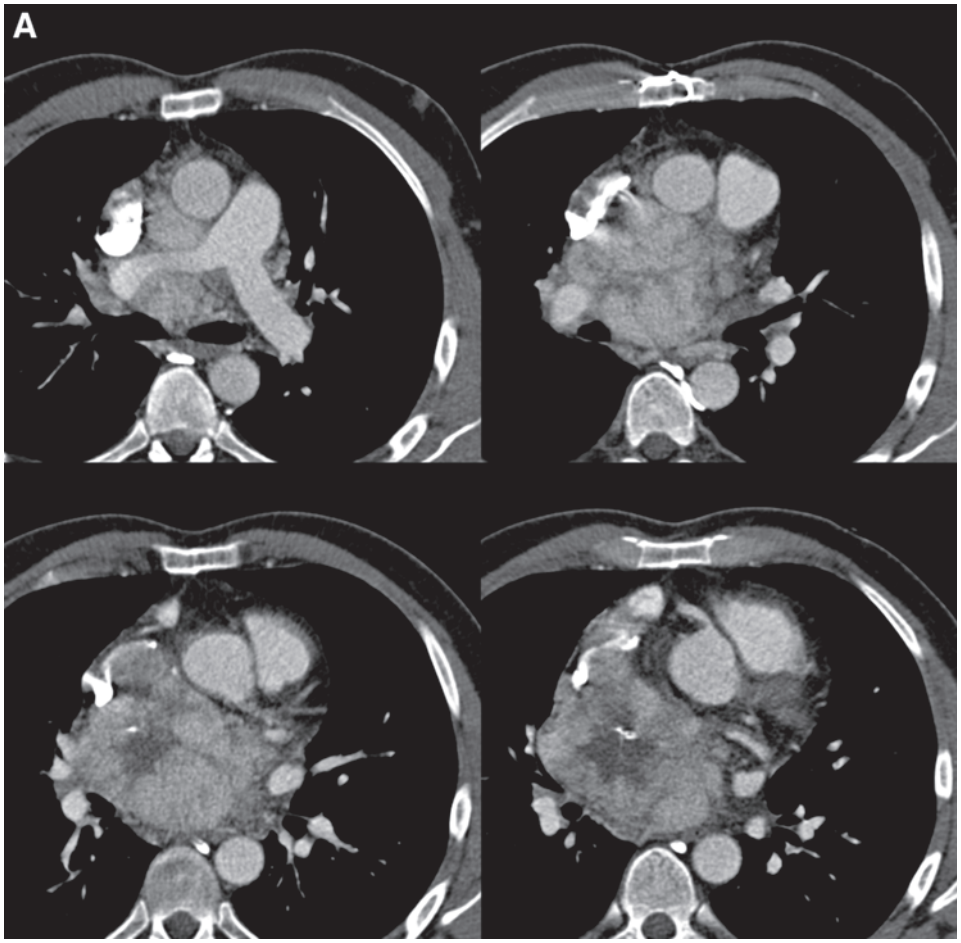
A

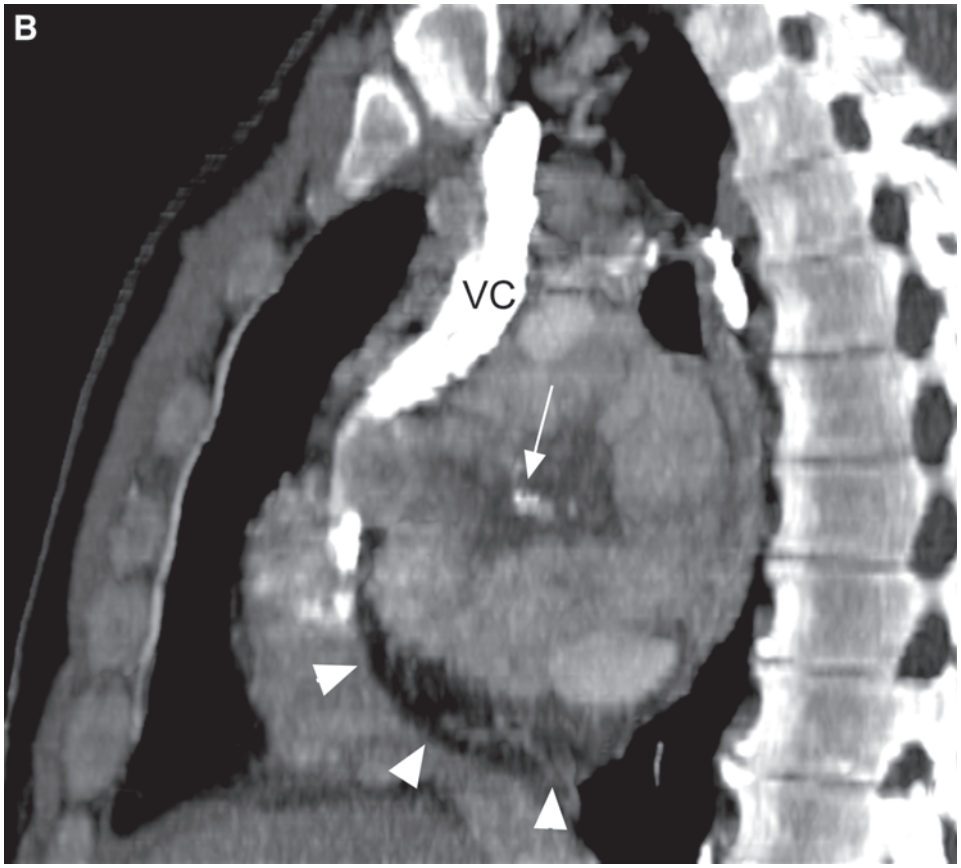
B
VC

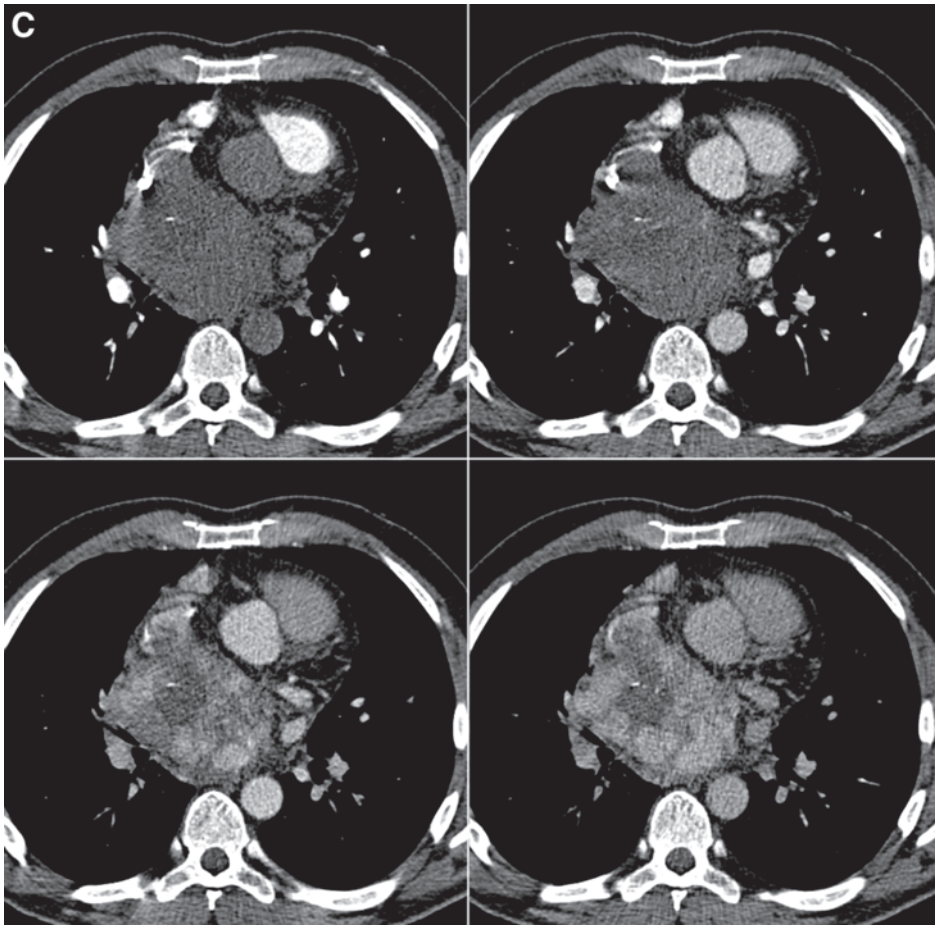

Fig. 5. *(Continued from page 174)* **(C)** Sequential electrocardiogram-triggered axial multidetector-row CT images at a constant level of the tumor shows a marked enhancement of most parts of the mass. This is based on the high degree of vascularization in this angiomyolipoma.

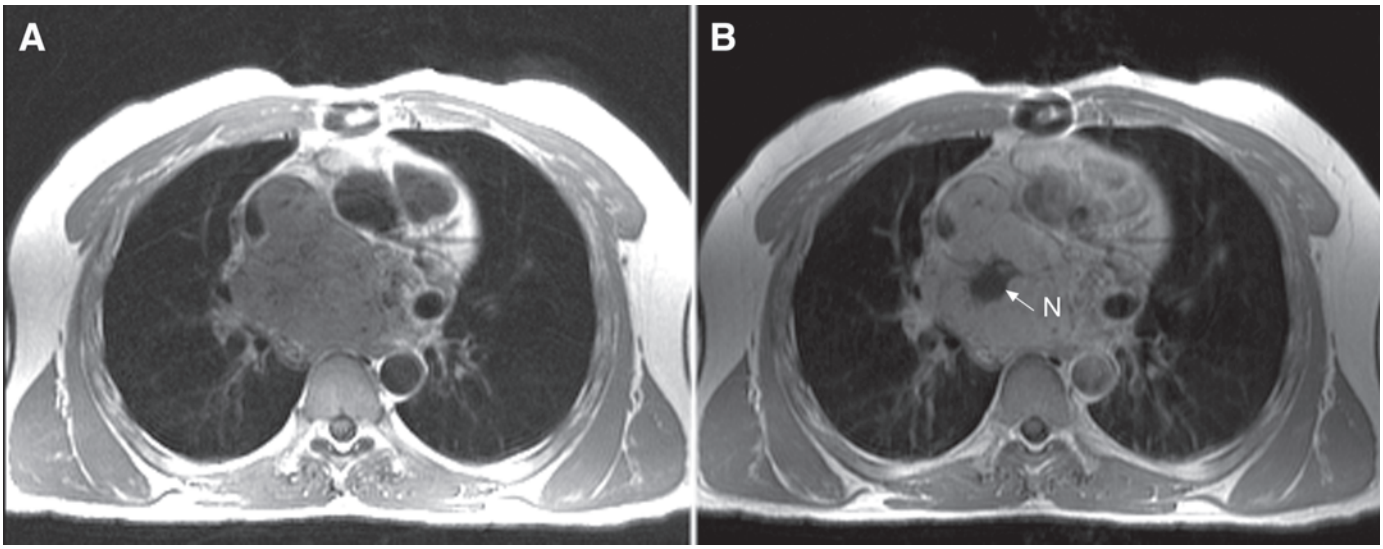

Fig. 6. Corresponding T1 weighted axial magnetic resonance imaging sections before **(A)** and after **(B)** contrast administration show massive enhancement of most tumor parts except a central necrosis (N).

sis have detectable cardiac masses *(24)*. Fibroma also primarily affects children and is often detected in infants or in utero by ultrasound *(25)*.

Beside these solid tumors, pericardial cysts represent a benign lesion that needs to be differentiated from other tumors.

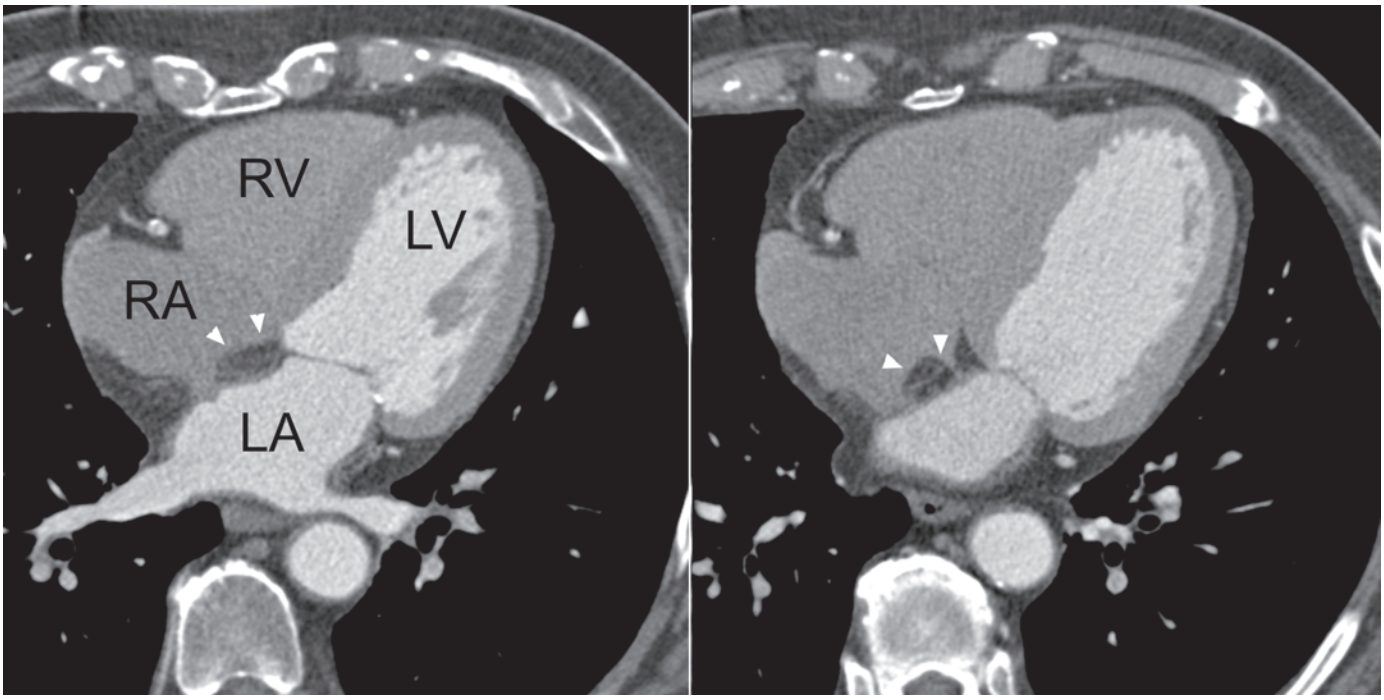

Fig. 7. Axial multidetector-row CT images of a patient with lipomateous hypertrophy of the atrial septum. Note the thickened septum and the low-density mass between both atria, consistent with fatty tissue (arrow heads). RA, right atrium; LA, left atrium; RV, right ventricle; LV, left ventricle.

MALIGNANT CARDIAC TUMORS

PRIMARY CARDIAC TUMORS

Primary cardiac malignancies are rather rare. Only 25% of all primary cardiac tumors are malignant *(13)*. In addition, they are much more uncommon than metastatic lesions to the heart. The distribution and frequency of different types varies within published data *(13)*. Primary cardiac malignancies represent a clinical dilemma. They are often asymptomatic until they become large, and even then they produce nonspecific symptoms *(26)*. Before the advent of cross-sectional imaging, primary cardiac malignancies were rarely diagnosed before death. Nowadays they are being diagnosed within living patients, allowing for conservative or even surgical treatment, including heart transplantation *(27)*. However, based on the usual delayed diagnosis of then extended disease including metastasis, these tumors show a rather bad outcome. CT can be used to accurately image the heart and the surrounding mediastinum, and therefore to evaluate the extent of disease.

Angiosarcoma represents the most common (approx 35–40%) cardiac sarcoma. Patients usually present with right-sided heart failure or tamponade based on its tendency to occur within the right atrium and to invade the pericardium (Fig. 8). Approximately 75% of angiosarcomas are located within the right atrium *(28)*. Based on their composition, they usually show a major contrast uptake, which may be combined with areas of necrosis. In contrast to angiosarcoma, rhabdomyosarcomas do not show a predominant location within the heart. On nonenhanced scans, they may show a density identical to normal myocardium, whereas they can usually be well differentiated from myocardium in enhanced scans. They may even invade cardiac valves, and tend to recur after resection (Fig. 9A,B). There are numerous other types of malignant primary cardiac tumors, including malignant fibrous histiocytomas, osteosarcomas, hemangiopericytomas, and lymphomas (Fig. 10). The approximate frequency of different types of malignant tumors is shown in Table 2.

Both CT and MRI are used in follow-up of malignant tumors after chemotherapy, resection, or even cardiac transplantation. When focusing on the primary lesion itself, cardiac gating is recommended, whereas in examinations for assessment of metastatic lesions from primary cardiac tumors, nongated techniques are adequate. Compared to MRI, CT allows for a comprehensive appreciation of the primary lesion and possible tumor spread with a single injection of contrast agent. Beside time-saving considerations, work-flow and patient management have to be taken into account

SECONDARY CARDIAC TUMORS

Secondary malignancies are 20–40 times more frequent than primary ones. As already mentioned, not only metastatic disease but also direct tumor involvement and invasion of the heart from primary lesions adjacent to the heart account for these cases. In addition to direct invasion, tumor spread to the heart can also arise via predefined venous structures, from hepatocellular carcinomas or renal cell carcinomas, for example. Based on their proximity to the heart, the most common tumors affecting the heart by direct invasion are bronchogenic carcinomas and breast tumors. An overview of the frequency of cardiac or pericardial involvement of different tumor types is given in Table 3. Imaging features of secondary cardiac malignancies are often but not mandatory, similar to those of the primary lesion.

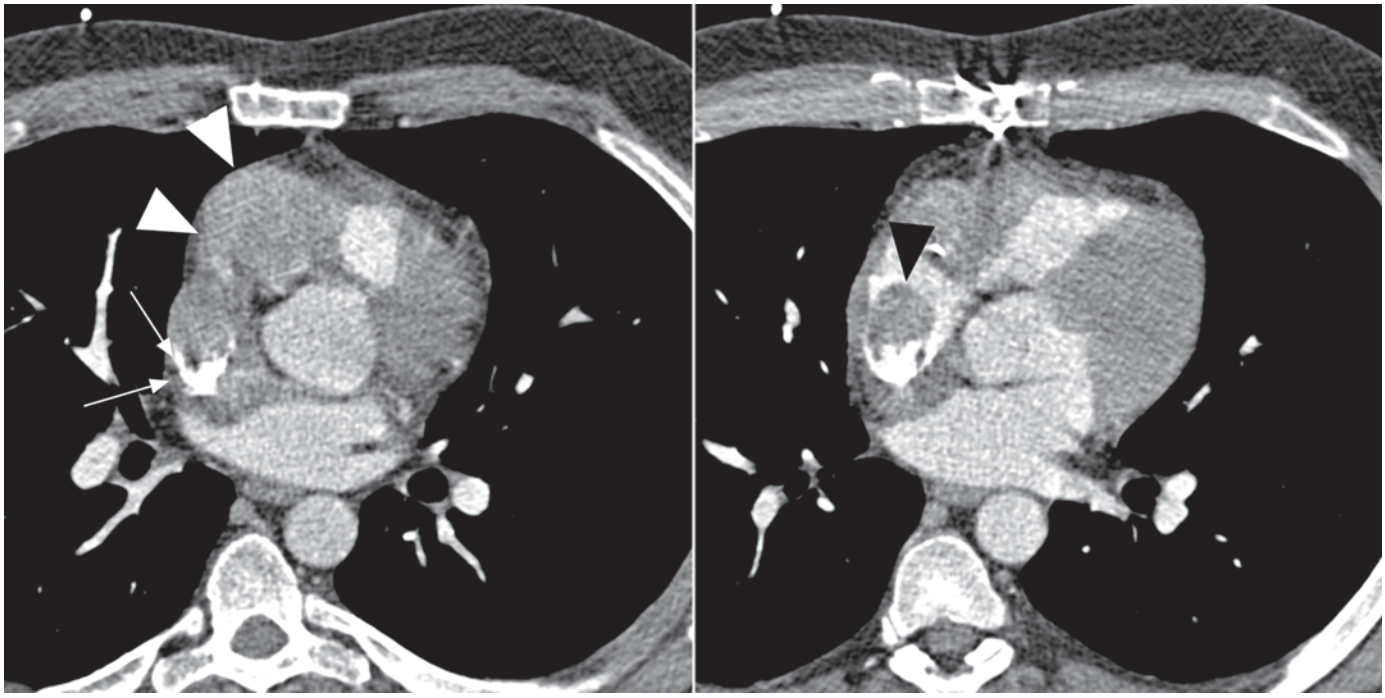

Fig. 8. Multidetector-row CT images of a patient with recurrent angiosarcoma involving the right atrium and parts of the right ventricle (arrow heads). The mass almost occludes the superior vena cava (arrows).

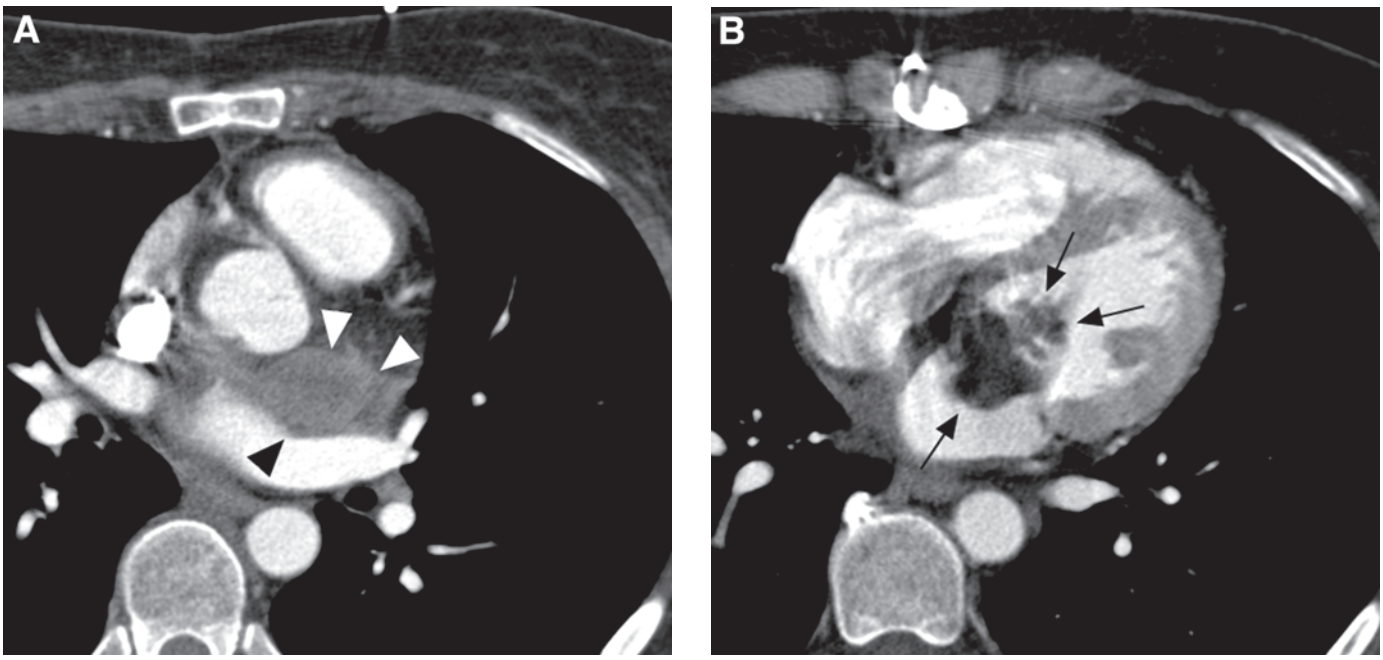

Fig. 9. (A) Recurrence of a rhabdomyosarcoma within the left atrium (arrow heads). **(B)** In addition to the tumor within the left atrium, the mass infiltrates the mitral valve and extends to the left ventricle (arrows).

IMAGING OF CARDIAC THROMBI

Thrombotic deposits within the heart are often referred to as pseudotumors or pseudomasses. Intracardiac thrombi may be caused by a variety of different pathologies and may occur in any cardiac chamber. They are responsible for approx 15% of all ischemic strokes and put patients at a major risk of stroke. Therefore, early identification with subsequent therapy is of paramount importance.

Occurring in virtually any part of the vascular system, the development of thrombotic clots may be based either on changes of surface properties, flow dynamics, or changes in blood coagulation. Patients with artificial devices (e.g., pros-

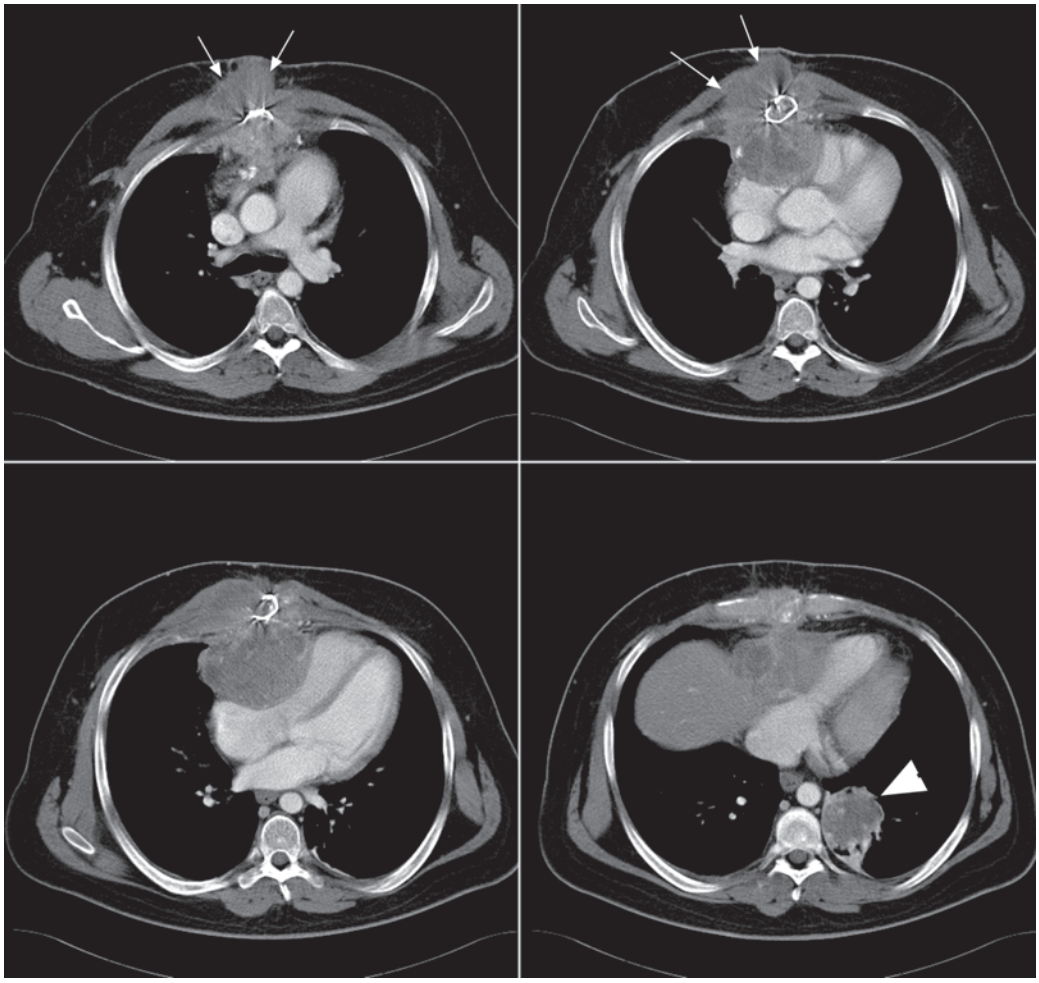

Fig. 10. A set of axial multidetector-row CT images of a malignant hemangiopericytoma involving the right coronary artery and the chest wall (arrows). The tumor encases the right atrium and ventricle. Within the left lower lobe of the lungs, metastatic disease in shown.

Table 2
Distribution and Frequency of Primary Cardiac Malignancies (adapted from ref. *13*)

Malignant tumors	*Approximate frequency (%)*
Angiosarcoma	9
Malignant fibrous histiocytoma	4
Osteosarcoma	3
Leimyosarcoma	3
Rhabdomyosarcoma	2
Lymphoma	2
Others	14
Total	37

Table 3
Frequency of Cardiac/Pericardial Involvement in Cases of Extracardiac Malignancies (adapted from ref. *13*)

Malignant tumors	*Frequency (%)*
Melanoma	49
Germinoma	42
Leukemia	34
Bronchogenic carcinoma	28
Sarcomas	22
Lymphomas	21
Breast Cancer	20
Esophageal carcinoma	17
Renal cell carcinoma	15
Thyroid carcinoma	12

thetic valves, pacemakers), atrial fibrillation, or wall motion abnormalities (including ventricular aneurysms) are at special risk. As already stated, thrombotic layers may also occur at the surface of myxomas or papillary fibroelastomas.

Thrombi may be solitary or multiple, and present as filling defects within opacified cardiac chambers. Their appearance depends on location. In regions of wall motion, abnormalities, or ventricular aneurysms after myocardial infarction, they usually lie adjacent to the areas of infracted myocardium. They can usually be differentiated from normal myocardium based on their rather low attenuation. However, in close contact to scar tissue in chronic infarction, the exact extent may be overesti-

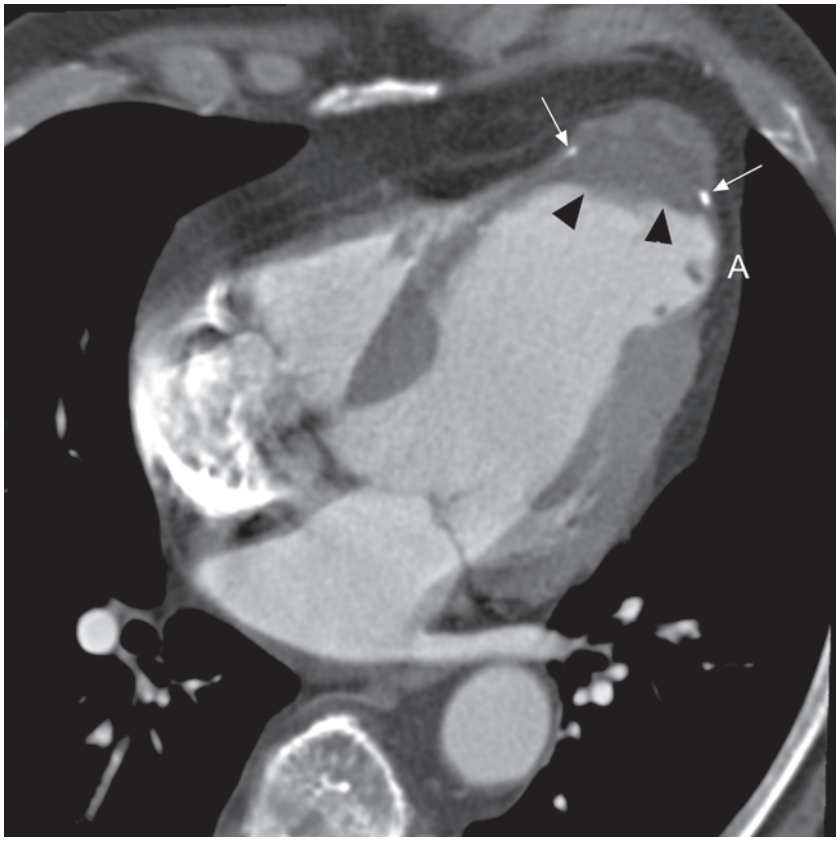

Fig. 11. Four-chamber view of a multidetector-row CT data set. Ventricular aneurysm (A) within the apex after myocardial infarction and a thrombus can be delineated (arrow heads). The thrombus show tiny calcifications (arrows).

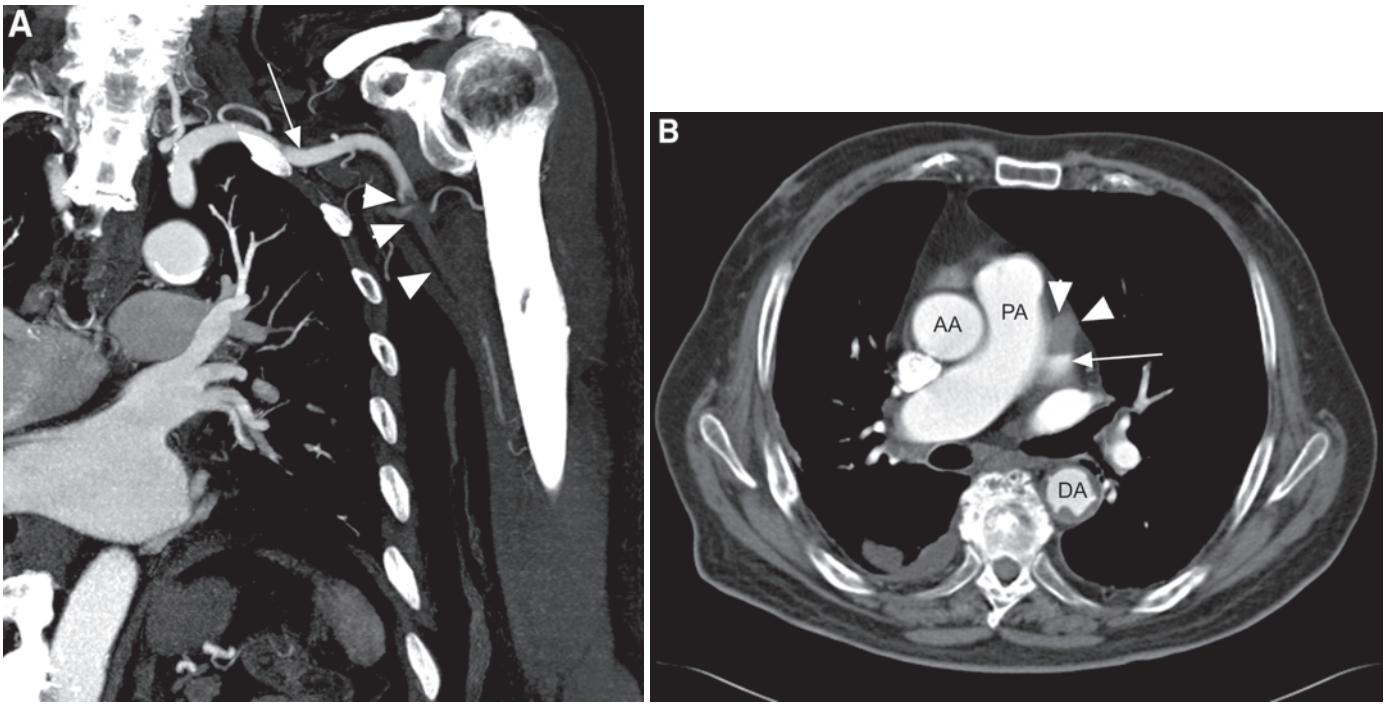

Fig. 12. (A) Multiplanar reformation (MPR) of the left upper extremity with an acute embolic occlusion of the axillary artery (arrow heads). The subclavian artery shows normal diameter and patency (arrow). **(B)** Reconstruction of the same data set focused in the chest shows residual thrombus (arrow heads) within the left atrial appendage (arrow). AA, ascending aorta; DA, descending aorta; PA, pulmonary artery.

mated. Long-standing thrombi tend to get organized and may calcify (Fig. 11). Clots within the atria are commonly related to contraction abnormalities (e.g., atrial fibrillation). They may often be found within the atrial appendages (Fig. 12A,B).

Echocardiography represents the basic modality for thrombus screening. However, based on the large field of view, cardiac CT allows for reliable depiction or occlusion of thrombi. Although not primarily used for cardiac imaging, routine CT of the chest may reveal unknown cardiac thrombi.

CONCLUSION

Cardiac CT shows promise in the assessment of cardiac masses. Especially with the widespread use of MDCT, this modality is rapidly growing in cardiac imaging. Its use in imaging of cardiac masses and thrombi represents only a niche indication. However, the requirements are less demanding than those of coronary CT angiography and can also be performed with less sophisticated MDCT scanner generations. However, as a prerequisite for cardiac CT imaging, ECG-based data acquisition strategies and algorithms are necessary. With the use of MDCT, a new modality of cardiac imaging competes with MRI. The acquisition of 3D data sets even allows for multiplanar imaging of cardiac tumors. There are specific features of tumors (e.g., calcifications) that may be visualized and depicted only in CT. On the other hand, CT may be inferior to MRI in exact evaluation of the tumor type in most cases, based on its lower soft-tissue contrast properties.

REFERENCES

1. Knez A, Becker CR, Leber A, et al. Usefulness of multislice spiral computed tomography angiography for determination of coronary artery stenoses. Am J Cardiol 2001;88:1191–1194.
2. Nieman K, Oudkerk M, Rensing BJ, et al. Coronary angiography with multi-slice computed tomography. Lancet 2001;357:599–603.
3. Nieman K, Cademartiri F, Lemos PA, Raaijmakers R, Pattynama PM, de Feyter PJ. Reliable noninvasive coronary angiography with fast submillimeter multislice spiral computed tomography. Circulation 2002;106:2051–2054.
4. Ropers D, Baum U, Pohle K, et al. Detection of coronary artery stenoses with thin-slice multi-detector row spiral computed tomography and multiplanar reconstruction. Circulation 2003;107: 664–666.
5. Felner JM, Knopf WD. Echocardiographic recognition of intracardiac and extracardiac masses. Echocardiography 1985;2:3.
6. Salcedo EE, Cohen GI, White RD, Davison MB. Cardiac tumors: diagnosis and management. Curr Probl Cardiol 1992;17:73–137.
7. Link KM, Lesko NM. MR evaluation of cardiac/juxtacardiac masses. Top Magn Reson Imaging 1995;7:232–245.
8. Olson LJ, Tajik AJ. Valvular heart disease. In: Skorton DJ, Schelbert HR, Wolf GL, Brundage BH. (eds.) Cardiac Imaging. 2nd ed. Saunders Company, Philadelphia: 1996;365–394.
9. MacMillan RM. Magnetic resonance imaging vs. ultrafast computed tomography for cardiac diagnosis. Int J Card Imaging 1992;8: 217–227.
10. Wintersperger BJ, Nikolaou K, Jakobs TF, Reiser MF, Becker CR. Cardiac multidetector-row computed tomography: initial experience using 16 detector-row systems. Crit Rev Comput Tomogr 2003;44: 27–45.
11. Wintersperger BJ, Becker CR, Gulbins H, et al. Tumors of the cardiac valves: imaging findings in magnetic resonance imaging, electron beam computed tomography, and echocardiography. Eur Radiol 2000;10:443–449.
12. Jakobs TF, Becker CR, Ohnesorge B, et al. Multislice helical CT of the heart with retrospective ECG gating: reduction of radiation exposure by ECG-controlled tube current modulation. Eur Radiol 2002;12:1081–1086.
13. Burke A, Virmani R. Tumors of the heart and great vessels. Armed Forces Institute of Pathology; Washington D.C.: 1995.
14. Carney JA, Gordon H, Carpenter PC, Shenoy PV, Go VL. The complex of myxomas, spotty pigmentation and endocrine overactivity. Medicine 1985;64:270–283.
15. Casey M, Mah C, Merliss AD, et al. Identification of a novel genetic locus for familial cardiac myxomas and Carney complex. Circulation 1998;98:2560–2566.
16. Burke AP, Virmani R. Cardiac myxomas: a clinicopathologic study. Am J Clin Pathol 1993;100:671–680.
17. Tsuchiya F, Kohno A, Saitoh R, Shigeta A. CT findings of atrial myxoma. Radiology 1984;151:139–143.
18. Abu Nassar SG, Parker JC, Jr. Incidental papillary endocardial tumor. Its potential significance. Arch Pathol 1971;92:370–376.
19. Willmann JK, Kobza R, Roos JE, et al. ECG-gated multi-detector row CT for assessment of mitral valve disease: initial experience. Eur Radiol 2002;12:2662–2669.
20. Willmann JK, Weishaupt D, Lachat M, et al. Electrocardiographically gated multi-detector row CT for assessment of valvular morphology and calcification in aortic stenosis. Radiology 2002;225:120–128.
21. Kamiya H, Ohno M, Iwata H, et al. Cardiac lipoma in the interventricular septum: evaluation by computed tomography and magnetic resonance imaging. Am Heart J 1990;119:1215–1217.
22. Hayashi H, Wakabayashi H, Kumazaki T. Ultrafast computed tomography diagnosis of an epicardial lipoma in the pericardial sac: the split pericardium appearance. J Thorac Imaging 1996;11: 161–162.
23. Smythe JF, Dyck JD, Smallhorn JF, Freedom RM. Natural history of cardiac rhabdomyoma in infancy and childhood. Am J Cardiol 1990;66:1247–1249.
24. Smith HC, Watson GH, Patel RG, Super M. Cardiac rhabdomyomata in tuberous sclerosis: their course and diagnostic value. Arch Dis Child 1989;64:196–200.
25. Beghetti M, Gow RM, Haney I, Mawson J, Williams WG, Freedom RM. Pediatric primary benign cardiac tumors: a 15-year review. Am Heart J 1997;134:1107–1114.
26. Araoz PA, Eklund HE, Welch TJ, Breen JF. CT and MR imaging of primary cardiac malignancies. Radiographics 1999;19:1421–1434.
27. Uberfuhr P, Meiser B, Fuchs A, et al. Heart transplantation: an approach to treating primary cardiac sarcoma? J Heart Lung Transplant 2002;21:1135–1139.
28. Janigan DT, Husain A, Robinson NA. Cardiac angiosarcomas: a review and a case report. Cancer 1986;57:852–859.